

Tracing Star Formation in Cool Core Clusters with GALEX

Amalia K. Hicks*, Richard F. Mushotzky^{†,**} and Megan Donahue*

**Department of Physics & Astronomy, Michigan State University, East Lansing, MI 48824-2320.*

[†]*Goddard Space Flight Center, Code 662, Greenbelt, MD, 20771.*

***Department of Astronomy, University of Maryland, College Park, MD 20742-2421.*

Abstract. We present recent results from a GALEX investigation of star formation in 16 cooling core clusters of galaxies, selected to span a broad range in both redshift and central cooling time. Initial results demonstrate clear UV excesses in most, but not all, brightest cluster galaxies in our sample. This UV excess is a direct indication of the presence of young massive stars and, therefore, recent star formation. We report on the physical extent of UV emission in these objects as well as their FUV-NUV colors, and compare GALEX inferred star formation rates to central cooling times, H α and IR luminosities for our sample.

Keywords: External galaxies and extragalactic objects: Origin, formation, evolution, age, and star formation; Astronomical Observations: Ultraviolet (10 – 300 nm)

PACS: 98.62.Ai; 95.85.Mt

INTRODUCTION

Despite past evidence of star formation in “cooling flow” (hereafter referred to as CF) clusters [e.g., 1, 2] the fact that star formation rate (SFR) estimates differed drastically from inferred X-ray cooling rates led to doubt that the two phenomena were related. However, recent UV investigations [3, 4], Spitzer data [5, 6], and precision optical photometry [7] have definitively shown that CF clusters are the sites of star formation, and that there is an indisputable relationship between X-ray properties and SFRs. Here we confirm and quantify this connection, using GALEX observations of a sample of 16 CF clusters.

SAMPLE AND OBSERVATIONS

The Galaxy Evolution Explorer (GALEX) is a space telescope with both imaging and spectroscopic capabilities in two ultraviolet wavebands, Far UV (FUV) 1350 – 1780 Å and Near UV (NUV) 1770 – 2730 Å [8]. Our GALEX targets consist of 16 clusters of galaxies that exhibit strong evidence of central cooling. These objects were chosen to cover a wide range in redshift ($0.02 < z < 0.45$) and central ($R = 20$ kpc) cooling time ($0.5 < t_{\text{cool}} < 2.5$ Gyr). Table 1 lists the objects in our sample, their redshifts, and GALEX exposure times. All of our targets were easily detected in both GALEX wavebands, with an average SNR of 40 (21) in the NUV (FUV), and minimum SNRs of ~ 6 in each band.

Cluster	z	Exposure (NUV/FUV) [s]	Cluster (cont.)	z (cont.)	Exposure (cont.)
Abell 85	0.0557	2494 / 2494	Hydra A	0.0549	2230 / 2230
Abell 1204	0.1706	3738 / 3738	MKW3s	0.0453	2271 / 2271
Abell 2029	0.0779	1517 / 1517	MKW4	0.0196	2194 / 2194
Abell 2052	0.0345	2863 / 2863	MS0839.8+2938	0.1980	4729 / 4728
Abell 2142	0.0904	1556 / 1556	MS1358.4+6245	0.3272	5614 / 5614
Abell 2597	0.0830	2111 / 2111	MS1455.0+2232	0.2578	3385 / 3384
Abell 3112	0.0761	4873 / 2618	RXJ1347.5-1145	0.4500	9120 / 9119
Hercules A	0.1540	3870 / 3870	ZwCl 3146	0.2906	3127 / 3127

IMAGING AND PHOTOMETRY

Surface brightness profiles in both wavebands were constructed for our targets in $5''$ bins (the approximate size of the larger PSF). Some of these profiles indicate UV emission at greater radii than had been previously detected. The SB profiles were then used to create radial color profiles. These tend to indicate pure star formation at small radii, then become progressively redder until, at large radii, colors are consistent with those of non-star forming ellipticals [9]. An example of each is shown in Figure 1.

Photometry was performed in $7''$ radius apertures centered on each BCG. This aperture size was chosen for compatibility with readily available 2MASS photometry. Using multiple archival GALEX observations, a control sample of 24 quiescent cluster ellipticals was obtained. These objects were used to construct a calibration relationship between UV and J band emission; effectively predicting the amount of UV light “expected” from a given old stellar population. This relationship was used to quantify the amount of “excess” UV light emitted by our CF sample (Figure 2). The majority of our sample exhibits clear UV excesses, indicating recent star formation.

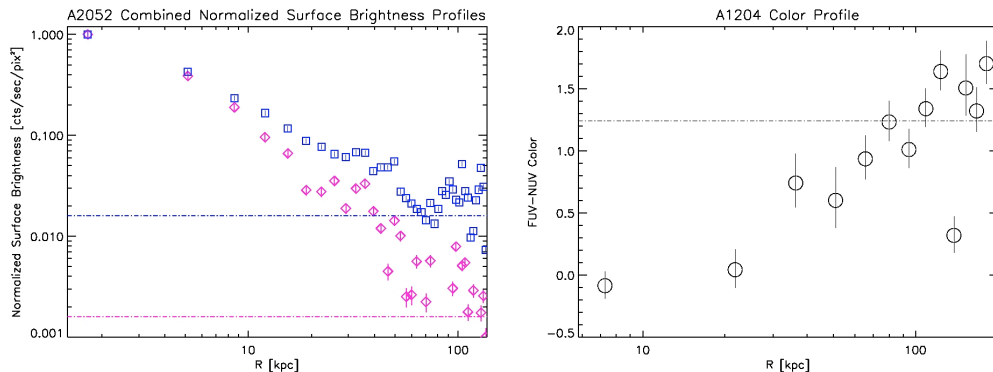


FIGURE 1. *Left (a):* UV surface brightness profiles for Abell 2052, normalized to a value of 1 in the central bin. The NUV profile is plotted with square symbols and FUV with diamonds. Horizontal lines indicate average NUV (top) and FUV (bottom) background levels. Note that UV emission (i.e., star formation) is detectable out to unprecedented radii with GALEX. *Right (b):* UV color profile (FUV-NUV) for Abell 1204, clearly showing bluer emission in the center. The horizontal line designates the color of the typical GALEX background. Star forming galaxies tend to have GALEX UV colors ~ 0.4 , while the majority (82%) of passively evolving elliptical galaxies have UV colors of > 0.9 [9].

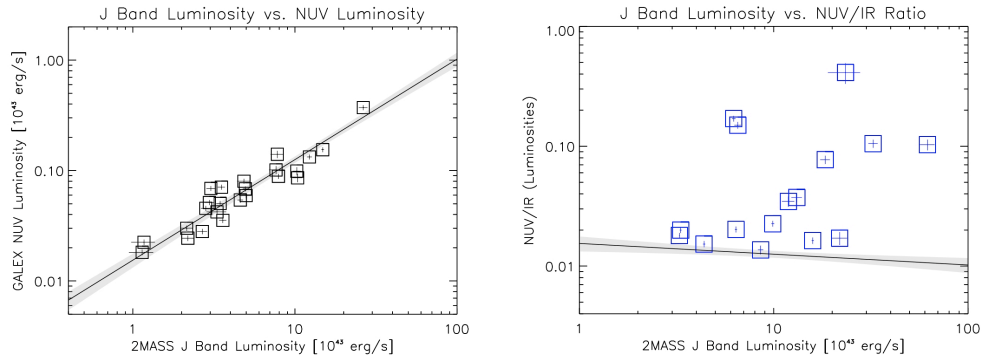


FIGURE 2. *Left (a):* NUV/J band calibration relationship obtained from 24 cluster ellipticals. *Right (b):* NUV/J vs. J band luminosity for our CF sample (squares). The line indicates the expected relationship for passively evolving ellipticals from our correlation; shaded regions designate 1σ errors on the fit.

MULTIWAVELENGTH COMPARISONS

For comparative purposes only, we translated our UV excesses into star formation rates using a Starburst99 model for continuous star formation over 20 Myr [10]. This timescale was chosen to grossly approximate episodic cooling timescales (during which the system undergoes feedback processes with alternating heating and cooling cycles). These SFRs were then compared to cluster properties from the literature.

$H\alpha$ measurements for our sample were taken from [2, 11, 12], and are shown vs. UV inferred SFRs in Figure 3. The consistency between UV and $H\alpha$ inferred star formation rates is remarkable, despite the many assumptions and unknowns that plague such comparisons. Infrared fluxes came from [5, 13, 14, 15], and were converted to SFRs as in [6]. This comparison plot is also shown in Figure 3.

The X-ray properties of our sample come from [12, plus private comm.]. In Figure 4 we show UV inferred SFRs vs. both entropy and cooling time at 20 kpc from the cluster center. The correlation between UV SFR and cooling time proves conclusively that the star formation in these objects is directly related to cooling gas in the cluster cores.

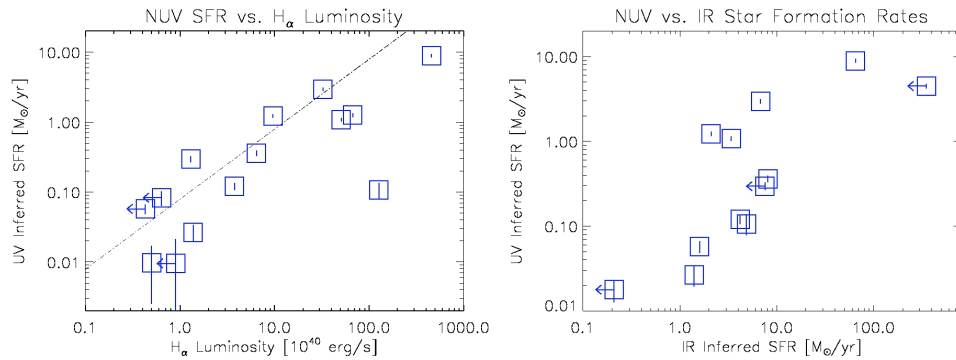


FIGURE 3. *Left (a):* UV inferred SFR vs. $H\alpha$ luminosity for a subset of our targets. The line indicates the $L_{H\alpha}$ -SFR relationship of [16]; *Right (b):* UV vs. IR inferred SFRs. A factor of ~ 10 discrepancy may suggest that star formation is highly obscured in our targets, however, this is unconfirmable at present due to the many assumptions inherent in SFR conversions in both wavebands.

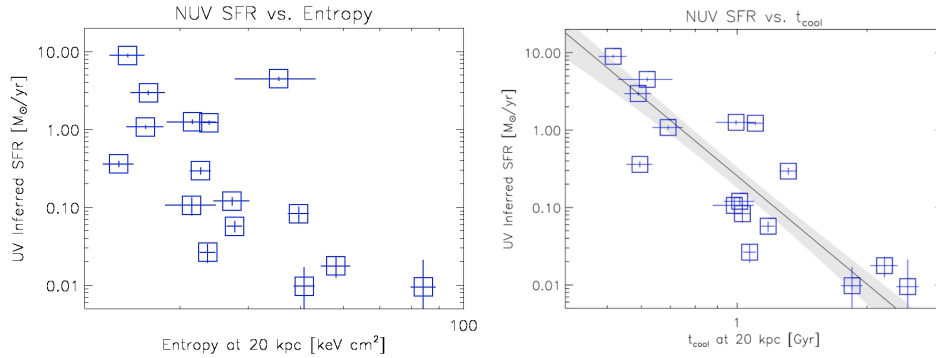


FIGURE 4. *Left (a):* UV inferred SFR vs. central gas entropy ($R = 20$ kpc), showing a tendency for more star formation to occur in lower entropy objects. The outlying point is our highest- z cluster. *Right (b):* UV inferred SFR vs. central cooling time ($R = 20$ kpc). A line shows the best BCES regress bisector fit, with a slope of -4.7 ± 0.5 . The shaded region designates 1σ errors on the fit.

SUMMARY

GALEX easily detects star formation in cluster BCGs out to $z \geq 0.45$ and to unprecedented radii. In most of the CF clusters studied, we find significant UV luminosity excesses and colors in the central galaxies that together suggest recent and/or current star formation. This finding is corroborated by $H\alpha$ and IR observations. A correlation between UV excess and central cooling time confirms that this star formation is directly and incontrovertibly related to the cooling gas.

ACKNOWLEDGMENTS

Support for this work was provided by NASA through GALEX award NNX07AJ38G and LTSA grant NNG05GD82G.

REFERENCES

1. B. R. McNamara, and R. W. O’Connell, *Astronomical Journal*, **98**, 201 (1989).
2. C. S. Crawford et al. , *Mon. Not. R. Astron. Soc.*, **306**, 857 (1999).
3. J. P. D. Mittaz et al. , *Astronomy & Astrophysics*, **365**, 93 (2001).
4. A. K. Hicks, and R. F. Mushotzky, *Astrophysical Journal Letters*, **635**, L9 (2005).
5. A. C. Quillen et al. , *Astrophysical Journal Supplement Series*, **176**, 39 (2008).
6. C. P. O’Dea et al. , *Astrophysical Journal*, **681**, 1035 (2008).
7. C. Bildfell et al. , *Mon. Not. R. Astron. Soc.*, **389**, 1637 (2008).
8. D. C. Martin et al. , *Astrophysical Journal Supplement Series*, **619**, 1 (2005).
9. A. Gil de Paz et al. , *Astrophysical Journal Supplement Series*, **173**, 185 (2007).
10. C. Leitherer et al. , *Astrophysical Journal*, **123**, 3 (1999).
11. M. Donahue, J. T. Stocke, and I. M. Gioia, *Mon. Not. R. Astron. Soc.*, **385**, 49 (1992).
12. K. W. Cavagnolo et al. , *Astrophysical Journal Supplement Series*, **182**, 12 (2009).
13. A. C. Edge, *Mon. Not. R. Astron. Soc.*, **328**, 762 (2001).
14. E. Egami et al. , *Astrophysical Journal*, **647**, 922 (2006).
15. M. Donahue et al. , *Astrophysical Journal*, **670**, 231 (2007).
16. R. C. Kennicutt, *Annual Review of Astronomy and Astrophysics*, **36**, 189 (1998).